



HAL
open science

Temperature dependent kinetic study of the gas phase reaction of ozone with 1-penten-3-ol, cis-2-penten-1-ol and trans-3-hexen-1-ol: Experimental and theoretical data

Carmen Kalalian, G. El Dib, H.J. Singh, P.K. Rao, Estelle Roth, Abdelkhaleq Chakir

► To cite this version:

Carmen Kalalian, G. El Dib, H.J. Singh, P.K. Rao, Estelle Roth, et al.. Temperature dependent kinetic study of the gas phase reaction of ozone with 1-penten-3-ol, cis-2-penten-1-ol and trans-3-hexen-1-ol: Experimental and theoretical data. *Atmospheric Environment*, 2020, 223, pp.117306. 10.1016/j.atmosenv.2020.117306 . hal-02472864

HAL Id: hal-02472864

<https://univ-rennes.hal.science/hal-02472864>

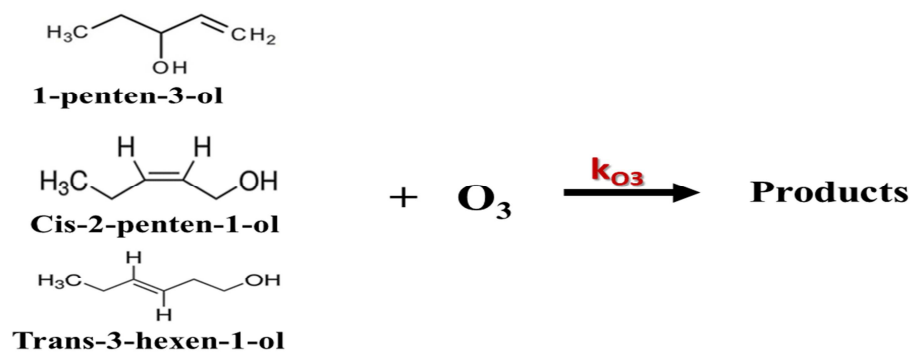
Submitted on 26 May 2020

HAL is a multi-disciplinary open access archive for the deposit and dissemination of scientific research documents, whether they are published or not. The documents may come from teaching and research institutions in France or abroad, or from public or private research centers.

L'archive ouverte pluridisciplinaire **HAL**, est destinée au dépôt et à la diffusion de documents scientifiques de niveau recherche, publiés ou non, émanant des établissements d'enseignement et de recherche français ou étrangers, des laboratoires publics ou privés.

C.K. performed the experimental measurements to determine the experimental rate constants. G.E.D., H.J.S., P.K.R. performed the theoretical calculations. E.R. and A.C. supervised the work. All authors participated in the data analysis and discussion and help editing the last version of the manuscript.

Journal Pre-proof



Journal Pre-proof

1 **Temperature dependent kinetic study of the gas phase reaction of ozone with 1-Penten-**
 2 **3-ol, Cis-2-penten-1-ol and Trans-3-hexen-1-ol: experimental and theoretical data**

3
 4 **C. Kalalian^{1*}, G. El Dib², H. J. Singh³, P. K. Rao³, E. Roth¹, A. Chakir^{1*}**

5
 6 ¹Groupe de Spectrométrie Moléculaire et Atmosphérique GSMA, UMR CNRS 7331, Université de Reims,
 7 Moulin de la Housse B.P. 1039, 51687 Reims Cedex 2.

8 ²Univ Rennes, CNRS, IPR (Institut de Physique de Rennes) -UMR 6251, F-35000 Rennes, France

9 ³Department of Chemistry, D.D.U. Gorakhpur University, Gorakhpur-273009, INDIA
 10

11 **Abstract**

12 C₅ and C₆ unsaturated alcohols are a family of biogenic volatile organic compounds (BVOC)
 13 emitted in the atmosphere from vegetation in response to their injuries. In this work, we
 14 report the first temperature dependent rate constants for the reaction of three unsaturated
 15 alcohols: 1-penten-3-ol (1P3OL), cis-2-penten-1-ol (c-2P1OL) and tran-3-hexen-1-ol (t-
 16 3H1OL) with ozone in a pyrex reactor coupled to a FTIR spectrometer and to a GC/MS at
 17 four different temperatures (273, 298, 313 and 333 K), at atmospheric pressure, using a
 18 relative method. The Arrhenius expressions obtained are (cm³ molecule⁻¹ s⁻¹):

1-Penten-3-ol : $k_{1P3OL+O_3} = (1.82 \pm 2.08) \times 10^{-16} \exp(- (730 \pm 348) / T)$

Cis-2-penten-1-ol : $k_{c-2P1OL+O_3} = (2.32 \pm 1.94) \times 10^{-15} \exp(- (902 \pm 265) / T)$

Trans-3-hexen-1-ol : $k_{t-3H1OL+O_3} = (1.74 \pm 1.65) \times 10^{-15} \exp(- (1020 \pm 300) / T)$

19 The studied reactions were also explored theoretically using computational methods based
 20 on quantum chemical theory characterizing the intermediates, transition states and the
 21 subsequent formation of reaction products. The rate constants were calculated at room
 22 temperature employing a modified transition-state theory (MTST). Both results obtained
 23 experimentally and theoretically, were discussed in terms of structure-reactivity
 24 relationships and temperature dependence. Tropospheric lifetimes of the investigated species
 25 with respect to ozone are calculated. The obtained results showed that these species are not
 26 persistent towards ozonolysis process.

27
 28 **Keywords:** biogenic volatile organic compounds (BVOC); unsaturated alcohols;
 29 ozonolysis; rate constants; DFT method, tropospheric lifetimes

^{1*} Corresponding authors: **Carmen KALALIAN**, carmenkalalian@hotmail.com; **Abdelkhaleq CHAKIR**, abdel.chakir@univ-reims.fr

30 1. Introduction

31 Unsaturated alcohols are a category of oxygenated BVOCs with an atmospheric
32 concentration of the order of few ppbv, particularly C₅ and C₆ unsaturated alcohols. Most
33 plants are affected by this type of emission caused by their wounds (Davis et al., 2007,
34 Grosjean et al., 1993, Grosjean and Grosjean, 1995, Lin et al., 2016). Hexenol and related
35 compounds give the green leaf odor when the lawn is mown or when the leaves begin to rot.
36 Hexenol can as well protect injured plants from pathogenic attack (Fuentes et al., 2000).
37 Moreover, several C₅ oxygenated compounds derived from α -linoleic acid can be emitted
38 from vegetation for microbiological protection purposes. These compounds include 1-
39 penten-3-ol and 2-penten-1-ol, emitted by various plants (Davis et al., 2007; Fisher et al.,
40 2003; Heiden et al., 2003; Karl et al., 2001; Kirstine et al., 1998). The emission of these
41 compounds by a wide variety of vegetation suggests that they are a significant source of
42 BVOCs in the atmosphere. It is therefore important to quantify their emission rate as well as
43 their atmospheric reactivity in order to evaluate their contribution to the formation of other
44 atmospheric oxidants.

45 In the atmosphere, in the gas phase, these unsaturated oxygenated BVOCs are likely to
46 be removed by reactions with atmospheric oxidants (OH, O₃, Cl and NO₃). Dry and wet
47 deposition pathways may also be considered. These atmospheric transformations generate
48 secondary pollutants namely photolabile carbonyl compounds, secondary organic aerosols
49 (SOA) and ozone production at regional and continental scales (Coates and Butler, 2015;
50 Jenkin and Hayman, 1999).

51 The atmospheric oxidation of unsaturated alcohols by OH radicals has been relatively
52 well studied (Davis and Burkholder, 2011; Gibilisco et al., 2013; Le Calvé et al., 2000;
53 Mellouki et al., 2003; Orlando et al., 2001; Papagni et al., 2009). However, studies of the
54 atmospheric degradation of unsaturated alcohols (> C₄) by ozone are scarce or non-existent,
55 especially those depending on temperature. To date, two studies concerning the ozonolysis
56 of a C₆ unsaturated linear alcohol, trans-3-hexen-1-ol exist in the literature and only at room
57 temperature (Gibilisco et al., 2015a; Lin et al., 2016). Gibilisco et al., (2015a) performed
58 their study in a 480L environmental chamber coupled to a FTIR spectrometer using the
59 relative method, while Lin et al., (2016) carried out their experiments in a 150L teflon
60 chamber coupled to GC/FID using the absolute mode. Moreover, the reactivity of two C₅
61 unsaturated alcohols, cis-2-penten-1-ol and 1-penten-3-ol, with ozone was studied by

62 Grosjean and Grosjean, (1994) and by O'Dwyer et al., (2010) at room temperature and at
63 atmospheric pressure, in the absolute mode using FTIR and GC/MS.

64 To complete the above studies and enrich the kinetic databases, we chose to evaluate
65 the rate constants of the ozonolysis of three unsaturated alcohols (1-penten-3-ol (1P3OL),
66 cis-2-penten-1-ol (c-2P1OL) and trans-3-hexen-1-ol (t-3H1OL) over the temperature range
67 of 273 to 333 K, at atmospheric pressure, in the presence of cyclohexane as an OH
68 scavenger, using the relative method. This study was performed in a 63L pyrex reactor
69 coupled to a FTIR spectrometer and to a GC/MS. To the best of our knowledge, this work
70 provides the first temperature-dependent kinetic study for the ozonolysis of 1-Penten-3-ol,
71 Cis-2-penten-1-ol, and Trans-3-hexen-1-ol.

72 The reactions of the unsaturated alcohols with ozone and the reaction sequence has
73 been also explored theoretically for the first time, using computational methods based on
74 quantum chemical theory characterizing the intermediates, transition states and the
75 subsequent formation of reaction products. The studied reactions are:



76

77 2. Experimental section

78 2.1. Experimental set-up

79 Kinetic measurements of the reactions of ozone with 1P3OL, c-2P1OL and t-3H1OL
80 were carried out in a 63 L tube, at four different temperatures: 273, 298, 313 and 333 K, at
81 atmospheric pressure, using a relative method. This device was described in detail in
82 previous studies from our laboratory and only a brief discussion will be given (Al Rashidi et
83 al., 2014; Kalalian et al., 2017; Laversin et al., 2016; Messaadia et al., 2013). In short, it is a
84 triple jacket Pyrex cell 200 cm long with an internal diameter of 20 cm, inside which there
85 are gold-coated mirrors to vary the optical path. The optical path used in this work was 56
86 m. A circulation of fluid (water or ethanol) between the first and the second jacket allows
87 working in a wide temperature range (233-373K). The pressure can vary between few mTorr
88 to 1000 Torr. This cell is coupled to a FTIR spectrometer (Bruker Equinox 55) operating in

89 the spectral range of 4000 to 400 cm^{-1} with a spectral resolution between 0.5 and 2 cm^{-1} as
90 well as to a GC/MS.

91 Ozone was generated using an ozonizer. The ozone generator consists of a double-
92 walled pyrex cylinder placed between two copper electrodes, connected to a KIKUSUI-
93 PCCR 500LE high frequency generator, having a single-phase output with a nominal
94 capacity of 500 VA. Ozone was produced by dissociation of oxygen flowing between the
95 two electrodes. The ozone-oxygen mixture was diluted with dry air at the exit of the
96 ozonizer and directed to a cylindrical Pyrex cell 12 cm in length, designed to measure in the
97 UV and thus control the amount of ozone introduced into the reactor tube. In our
98 experiments, ozone concentration was measured at 270 nm using an Avaspec CCD camera.

99 The studied alcohols and the references used were introduced into the reactor at
100 concentrations of $(0.40\text{-}1.00) \times 10^{15}$ molecules cm^{-3} . Cyclohexane, scavenger of OH
101 radicals likely to form in the reactor, was added at concentrations of $(10\text{-}50) \times 10^{15}$
102 molecules cm^{-3} . Once in the reactor, the ozone was then introduced with a continuous flow
103 of 0.1 mL/ min (corresponding to a concentration of the order of 10^{12} molecules cm^{-3}). The
104 used reference compounds were: 2,3-dimethyl-1,3-butadiene for the FTIR measurements
105 and 1-heptene or 1-penten-3-ol for the GC/MS measurements (example given in **Figure S-**
106 **1**).

107 For the FTIR measurements, IR spectra were recorded every 45 seconds. Each
108 spectrum is an accumulation of 30 spectra. The experiment lasts about one to three hours.
109 The IR bands specific to each of the compounds studied were integrated so there was no
110 overlap with the reference band and those of the reaction products formed. The integrated
111 bands were: 930 - 950 cm^{-1} for 1P3OL, 920 - 960 cm^{-1} for c-2P1OL, 939 - 987 cm^{-1} for t-
112 3H1OL and 1574 - 1631 cm^{-1} for the reference 2,3-dimethyl-1,3-butadiene.

113 In the case of the coupling with the GC/MS, an SPME fiber type polydimethylsiloxane
114 (PDMS) was used for sampling. This fiber was exposed for 1 minute into the reactor. A
115 sampling time of 1 minute seemed to be a good compromise between the characteristic time
116 of kinetics and the thermodynamic equilibrium. Samples were taken every 10 min
117 throughout the duration of the experiment.

118 The studied compounds were provided by Sigma Aldrich: 1-penten-3-ol (> 98 %), cis-
119 2-penten-1-ol (\geq 96 %), trans-3-hexen-1-ol (97 %), cyclohexane (\geq 99 %), 2,3-dimethyl-1,3-
120 butadiene (98 %), 1-heptene (97 %) and were used without further purification. As for the
121 gases, they were provided by Air Liquide: Air (> 99.9999 %), O_2 (> 99.999 %), He (>
122 99.999 %).

123 **2.2. Experimental data analysis**

124 The compound and the reference are simultaneously subjected to ozonolysis, their wall
 125 loss effect and other pseudo first-order reactions. The set of reactions that take place in the
 126 reactor are:



$$\frac{-d[\text{Alcohol}]}{dt} = k_{\text{O}_3} [\text{Alcohol}]_g [\text{O}_3]_g + k_p [\text{Alcohol}]_g \quad \text{(Eq.1)}$$



$$\frac{-d[\text{Reference}]}{dt} = k_{\text{ref}} [\text{Reference}]_g [\text{O}_3]_g + k'_p [\text{Reference}]_g \quad \text{(Eq.2)}$$

127 $[\text{Alcohol}]_g$ and $[\text{Reference}]_g$ are the alcohol and the reference concentrations, $[\text{O}_3]_g$ is
 128 the gas phase ozone concentration, k_p and k'_p are the sum of first order or pseudo first order
 129 rate constants due to wall losses as well as secondary reactions for the studied alcohols and
 130 the reference compound.

131 Integration of Eqs 1 and 2 leads to the following relation:

$$\frac{1}{t} \ln \left(\frac{[\text{Alcohol}]_0}{[\text{Alcohol}]_t} \right) = R \frac{1}{t} \ln \left(\frac{[\text{Reference}]_0}{[\text{Reference}]_t} \right) + (k_p - Rk'_p) \quad \text{(Eq.3)}$$

132 where $R = k_{\text{O}_3} / k_{\text{ref}}$, k_{O_3} and k_{ref} are the second order rate constants ($\text{cm}^3 \text{ molecule}^{-1} \text{ s}^{-1}$) of
 133 the alcohol and the reference with ozone, $[\text{Alcohol}]_0$ and $[\text{Reference}]_0$ are the alcohol and
 134 the reference initial concentrations at the initial time t_0 and $[\text{Alcohol}]_t$ and $[\text{Reference}]_t$ are
 135 that at reaction time t .

136 Since the unsaturated alcohols concentrations are proportional to the areas of the IR
 137 band or chromatographic peak, the plot of $1/t \ln (A_{0 \text{ alc}}/A_{\text{alc}})$ as a function of $1/t \ln (A_{0 \text{ ref}}/A_{\text{ref}})$
 138 $/A_{\text{ref}})$ is a straight line whose slope corresponds to the ratio $R = k_{\text{O}_3} / k_{\text{ref}}$, with $A_{0 \text{ alc}}$ and $A_{0 \text{ ref}}$
 139 ref corresponding to the areas of the alcohol and the reference bands at time t_0 and A_{alc} and

140 A_{ref} are that at time t . Multiplying this ratio by the rate constant of the known reference, k_{ref} ,
141 we can determine the second-order rate constants of the ozonolysis of the studied alcohols
142 k_{O_3} (in $\text{cm}^3 \text{ molecule}^{-1} \text{ s}^{-1}$). The ozonolysis reaction of the studied alcohols were repeated 3-
143 4 times for each temperature (273, 298, 313 and 333K).

144 3. Computational method

145 All the electronic structure calculations were carried out at an IBM Cluster using
146 Gaussian 09 suite of programs (Frisch et al., 2008). The geometry optimization of all the
147 species involved in the reactions considered, the intermediates and their subsequent
148 degradation products was carried out at DFT method using M06-2X functional in
149 conjunction with the triple split valence polarized basis set 6-311++G(d,p) with diffuse
150 functions added to heavy atoms. M06-2X functional is a meta hybrid density functional
151 which incorporates 54% of HF exchange and proposed to yield reliable thermochemical and
152 kinetic parameters involving main group elements when coupled with a suitably large basis
153 set (Zhao and Truhlar, 2006, 2008). Computation of harmonic vibrational frequencies was
154 made on the same level of theory to verify the nature of the corresponding stationary points.
155 All the stable species were classified as minima on the corresponding potential energy
156 surface (PES). These stable species were characterized by the presence of all real vibrational
157 frequencies. The transition states were located, and their existence was verified by the
158 presence of only one imaginary frequency along the transition vector. The frequency
159 calculations led to determine the electronic energy of the species concerned. Zero-point
160 vibrational energy (ZPVE) of the respective species was also calculated at M06-2X/6-
161 311++G(d,p) level and corrected by employing a correction factor of 0.95 (James et al.,
162 2011). In order to ascertain the occurrence of the transition state, Intrinsic Reaction
163 Coordinate (IRC) (Gonzalez and Schlegel, 1989) calculations in both directions (forward
164 and reverse) were made in order to see that the transition was smooth from reactants to
165 products via the transition state. IRC calculations were performed at the M06-2X/6-
166 311++G(d,p) level of theory using 12 points each in forward and reverse directions at 0.1
167 $\text{amu}^{1/2}$ -Bohr step size.

168 4. Results and Discussion

169 4.1. Determination of the rate constants experimentally

170 Rate constants of the reaction of ozone with 1P3OL, c-2P1OL and t-3H1OL were
 171 determined in the temperature range of 273 to 333 K, at atmospheric pressure, using the
 172 relative method. **Figs. 1-3** show the plots of $1/t \ln (A_{0\text{ alc}}/A_{\text{alc}})$ as a function of $1/t \ln (A_{0\text{ ref}}/A_{\text{ref}})$
 173 for the three unsaturated alcohols at different temperatures (273, 298, 313, 333K)
 174 obtained by FTIR (reference: 2,3-dimethyl-1,3-butadiene) and only at 298 K by SPME-
 175 GC/MS (reference: 1-heptene). Good linearity is observed with correlation coefficients (r^2)
 176 greater than 90% in accordance with **Eq. (3)**.

177 Ozonolysis rate constants, k_{O_3} , obtained experimentally by the two analytical
 178 techniques FTIR and SPME-GC/MS, are presented in **Table 1**. The overall uncertainties on
 179 the second-order rate constants, k_{O_3} , are calculated from the error propagation method at
 180 each temperature. The uncertainty is 14 to 18% for 1-penten-3-ol, 13 to 14% for cis-2-
 181 penten-1-ol and 15% for trans-3-hexen-1-ol.

182 In order to establish the Arrhenius relationship, $\ln k_{\text{O}_3}$ is plotted as a function of $1/T$
 183 for the three studied unsaturated alcohols (**Fig. 4**). The Arrhenius parameters can be deduced
 184 from the slope and the intercept. In the temperature range 273-333K, the Arrhenius
 185 expressions of the studied unsaturated alcohols ($\text{cm}^3 \text{ molecule}^{-1} \text{ s}^{-1}$) are:

1-Penten-3-ol : $k_{1\text{P3OL}+\text{O}_3} = (1.82 \pm 2.08) \times 10^{-16} \exp(- (730 \pm 348) / T)$

Cis-2-penten-1-ol : $k_{\text{c-2P1OL}+\text{O}_3} = (2.32 \pm 1.94) \times 10^{-15} \exp(- (902 \pm 265) / T)$

Trans-3-hexen-1-ol : $k_{\text{t-3H1OL}+\text{O}_3} = (1.74 \pm 1.65) \times 10^{-15} \exp(- (1020 \pm 300) / T)$

186 Uncertainties on the Arrhenius parameters (activation energy E_a and pre-exponential factor
 187 A) were calculated using the weighted least squares method.

188 4.2. Error analysis on experimental determinations

189 The overall error on the rate constants reported in this work arises from: (i) Random
 190 errors caused by unknown and unpredictable changes in the experiment that occur mainly in
 191 the measuring instruments. These errors are reduced by averaging several experiments and
 192 their contribution is lower than that of systematic errors. (ii) Systematic errors are due to

193 methodological, instrumental and personal errors. In this work, errors on the ozonolysis rate
 194 constants of unsaturated alcohols were determined using the error propagation:

$$195 \quad \Delta k_{O_3} = k_{O_3} \times \left[\left(\frac{\Delta k_{ref}}{k_{ref}} \right)^2 + \left(\frac{\Delta \left(\frac{k_{O_3}}{k_{ref}} \right)}{\frac{k_{O_3}}{k_{ref}}} \right)^2 \right]^{1/2} \quad (\text{Eq. 4})$$

196 Where $\Delta k_{ref} / k_{ref}$ and $\Delta (k_{O_3} / k_{ref}) / (k_{O_3} / k_{ref})$ are the relative errors on k_{ref} and k_{O_3} / k_{ref} ,
 197 respectively. The errors sources come mainly from:

- 198 • The error on k_{ref} : this value is given by the literature; it varies from 5 to 20%
 199 depending on the used reference.
- 200 • The error on the determination of the ratio k_{O_3} / k_{ref} : This parameter represents the
 201 slope of the plot $1/t \ln [\text{alcohol}]_0 / [\text{alcohol}]$ vs $1/t \ln [\text{ref}]_0 / [\text{ref}]$ determined directly
 202 from the experimental points. The error on this parameter is mainly influenced by the
 203 analytical technique used to track reagent concentrations. The uncertainty on the
 204 slope k_{O_3}/k_{ref} for the IR measurements mainly depends on errors related to the
 205 integration of the spectroscopic peak areas of the analyte and the reference. To
 206 minimize this error, 30 to 70 spectra were collected at different time intervals for
 207 each experiment. For SPME-GC/MS measurements, the experimental conditions are
 208 optimized such as the column temperature, the SPME fiber type, the exposure time
 209 in the reactor and the selection of the reference compound to have relatively intense
 210 chromatographic peaks. In addition, for each experiment, 3 to 4 runs were performed
 211 to minimize the error on the determination of the slope (k_{O_3}/k_{ref}). The uncertainty on
 212 this parameter was calculated by the least square's method.

213 **4.3. Electronic structure**

214 It is a well-established fact that reactions of ozone with alkenes occur by the
 215 cycloaddition of ozone to the C=C double bond (Rao and Gejji, 2018, 2017a). A very high
 216 level calculation performed on ozone addition at the simplest alkene C_2H_4 concluded that
 217 Criegee mechanism is more pertinent as compared to De Moore mechanism (Gadzhiev et
 218 al., 2012). As a result, we followed the kinetics of the reactions of the three unsaturated
 219 alcohols with ozone to the formation of the primary ozonide (POZ). Theoretical studies
 220 performed on ozonolysis of alkenes such as ethene and isoprene have shown that the
 221 activation energies for such reactions proceeds with negative activation barrier (Olzmann et
 222 al., 1997; Zhang and Zhang, 2002). This implies that cycloaddition of ozone is likely to

223 occur through a Van der Waals complex prior to the transition state. Therefore, the
224 possibility of involvement of pre-reactive complexes in the entrance channel of the
225 corresponding potential energy surface was considered in this work and the reaction under
226 the following reaction sequence was explored.

227 1P3OL (A), *c*-2P1OL (B) or *t*-3H1OL (C) + O₃ → [Complex, RC] → TS → Primary
228 Ozonide (POZ)

229 The optimized geometries of all the species involved in the reactions of A, B and C
230 with ozone are shown in **Fig. 5**. A few vital geometric parameters that are expected to be
231 more critical during the reaction process are also listed on the figure. The detailed positional
232 coordinates of the atoms in the optimized geometries of the species involved during
233 reactions are given the **Supplementary Material (Table S1)**. A detailed analysis of the
234 optimized structures of the complexes reveal that the two interacting C---O bond of the
235 complex were found to be in the range of 2.750 – 2.937 Å. Such a long distance shows that
236 the complexes are indeed a weak complex of the Van der Waals type.

237 The transition states possessed only one imaginary harmonic vibrational frequency as
238 280 *i*, 219 *i* and 248 *i* for transition states TS_A, TS_B and TS_C respectively (**Supplementary**
239 **Material -Table S2**) and can be classified as the first-order saddle point. The energy
240 profiles of the reactions of A, B and C with ozone are made with the zero-point corrected
241 energy values obtained during frequency calculation and these are shown in **Fig. 6**. The
242 computed energy values of the species concerned along with their zero-point energies are
243 given in **Supplementary Material (Table S2)**. In constructing the profiles, the energy
244 values are presented with respect to the reactant molecules set to zero. The results show that
245 the calculated energy difference between the transition states and the reactants in reactions
246 of O₃ with A, B and C are 0.16, -3.72 and -2.65 kcal/mol, respectively. Thus, we find that
247 the cycloaddition of ozone on the species A is almost without barrier whereas on B and C it
248 proceeds with a negative barrier. It is known that reactions occurring with negative
249 activation barrier proceeds with the formation of pre-reactive complexes (Li et al., 2015;
250 Olzmann et al., 1997; Rao and Gejji, 2017a, 2017b; Xie et al., 2015; Zhang and Zhang,
251 2002). A rigorous search for stable minima in the entrance channel of the respective
252 potential energy surface was therefore performed. During the search on a relaxed PES the
253 stable minima RC_A, RC_B and RC_C corresponding to each reaction were found whose
254 optimized geometries are also shown in **Fig. 5**. The energy profiles plotted in **Fig. 6** show
255 that the pre-reaction complexes are stabilized by an energy of the amount of 3.72, 5.09 and

256 5.25 kcal/mol with respect to the corresponding reacting species in reactions with A, B and
 257 C, respectively. In order to confirm that the reactions proceeded through a pre-reactive
 258 complex, the IRC calculations performed at M06-2X/6-311++G(d,p) level of theory along
 259 the reaction path in both the directions of the transition state as shown in **Fig. 7** were
 260 analyzed. The analysis showed that the reactant side indeed represented the vdW and the
 261 transition from vdW to the primary ozonides was smooth.

262 **4.4. Thermochemical analysis and Rate Constants**

263 The reaction energies involved during the reaction of ozone with A, B and C are
 264 calculated. The results show that the formation of primary ozonides are highly exothermic
 265 (ΔH_{298}^0 : A + O₃ = -74.76; B + O₃ = -76.56 and C + O₃ = -72.84 kcal/mol and highly
 266 exothermic with the respective ΔG_{298}^0 values of -61.08, -61.29 and -59.27 kcal/mol). This
 267 shows that the formation of primary ozonide is spontaneous and the most probable one.

268 The entrance channel of the potential energy surface (PES) is attractive and this leads
 269 to the formation of weak Van der Waals complexes for reactions of ozone with titled
 270 alcohols. The reaction under such a circumstance occurs with a negative activation barrier.
 271 The reaction complex further proceeds to form primary ozonide through the transition state.
 272 During the present study a modified transition state theory (MTST) was employed to
 273 calculate the rate constants of the reactions considered (Krasnoperov et al., 2006). It is
 274 assumed that the reactions with negative energy barrier proceed in two steps. In the first
 275 step, reactants form a complex, which is in microcanonical equilibrium with the reactant
 276 molecules at all energy levels and the reaction occurs with the following sequence:



278 In the above reaction sequence, R₁ is A, B or C and R₂ is O₃. In the second step, the
 279 reaction complex decomposes to yield the reaction products and this step is the rate
 280 controlling step. Thus, the overall rate of the bimolecular reaction can be written as

$$281 \quad \text{Rate} = k_{\text{RC}} [\text{RC}] \quad (\text{Eq.5})$$

282 Where k_{RC} is the unimolecular rate of decomposition of the reaction $\text{RC} \rightarrow \text{Products}$ and is
 283 given by the equation:

$$284 \quad k_{\text{RC}} = \Gamma(T) \sigma \frac{k_{\text{b}} T}{h} \frac{Q_{\text{TS}}}{Q_{\text{RC}}} e^{-\frac{(E_{\text{TS}} - E_{\text{RC}})}{RT}} \quad (\text{Eq. 6})$$

285 In the above equation, $\Gamma(T)$ is the tunneling correction factor at a temperature T , σ is the
 286 reaction path degeneracy, k_b is Boltzmann's constant, T is temperature, h is Planck's
 287 constant, Q_{TS} and Q_{RC} are the molecular partition functions of the transition-state and the
 288 reaction complex respectively, $(E_{TS} - E_{RC})$ is the energy barrier between the transition-state
 289 and the reaction complex and R is the universal gas constant.

290 The unimolecular rate constant, k_{RC} can be calculated theoretically utilizing the
 291 quantum chemical methods by computing the partition functions of the transition state and
 292 the pre-reactive complex and the activation barrier $E_{TS} - E_{RC}$. Since the pre-reactive
 293 complex RC is statistically in equilibrium with the reacting species at all energy levels, the
 294 equilibrium concentration of the complex, RC can be calculated utilizing the statistical
 295 mechanical theory and can be written as

$$296 \quad [RC] = \frac{Q_{RC}}{Q_{R1} \cdot Q_{R2}} [R_1][R_2] \quad (\text{Eq. 7})$$

297 Where Q_{R1} , Q_{R2} and Q_{RC} are the molecular partition functions of the reacting species and the
 298 complex. Thus, the rate of bimolecular reaction can be written as:

$$299 \quad \text{Rate} = k_{RC} [RC] = k_{RC} \cdot \frac{Q_{RC}}{Q_{R1} \cdot Q_{R2}} [R_1][R_2] \quad (\text{Eq. 8})$$

300 Hence, the effective bimolecular rate constant is given by $k_{RC} \frac{Q_{RC}}{Q_{R1} \cdot Q_{R2}}$. The reaction path
 301 degeneracy σ is generally taken to be unity for the unimolecular reactions. The tunneling
 302 correction factor $\Gamma(T)$ has been estimated using Wigner's method (Wigner, 1932) and this
 303 has been found to be very close to unity in each of the reactions considered during the
 304 present study. Thus, concluded that tunneling is insignificant during the reactions
 305 considered. The calculated bimolecular rate constants of the reactions considered during the
 306 present investigation come out to be : (A) + O₃, $0.2 \times 10^{-17} \text{ cm}^3 \text{ molecule}^{-1} \text{ s}^{-1}$; (B) + O₃,
 307 $1.48 \times 10^{-17} \text{ cm}^3 \text{ molecule}^{-1} \text{ s}^{-1}$; (C) + O₃ $1.5 \times 10^{-17} \text{ cm}^3 \text{ molecule}^{-1} \text{ s}^{-1}$ having apparent
 308 activation energies of 3.88, 1.37 and 2.60 kcal/mol respectively. Although the computed
 309 activation energy of the reaction 1P3OL + O₃ is higher than the experimental one, the values
 310 for the other two reactions considered during the present study are quite comparable with the
 311 experimentally determined values (**Table 3**). As a result, the rate constants evaluated using
 312 quantum mechanical method for reactions of ozone with 1P3OL, c-2P1OL and t-3H1OL are
 313 on the average 6-7 times lower than that of the experimental values (**Table 1**). Moreover,
 314 these calculations have highlighted the formation of a pre-reaction complex that leads to an
 315 activated complex.

316 **4.5. Comparison with the literature**

317 Experimental rate constants for the reaction of ozone with 1P3OL, c-2P1OL and t-
318 3H1OL, determined in this work were compared with those found in the literature at room
319 temperature (**Table 1**). The average room temperature rate constants obtained in FTIR and
320 GC/MS are ($\times 10^{-17} \text{ cm}^3 \text{ molecule}^{-1} \text{ s}^{-1}$): (1.68 ± 0.32) for 1P3OL, (10.50 ± 1.99) for c-2P1OL
321 and (6.24 ± 1.37) for t-3H1OL. Grosjean and Grosjean (1994) studied the kinetics of
322 ozonolysis of 1P3OL and c-2P1OL using the absolute method and reported an ozonolysis
323 rate constant of (1.79 ± 0.18) $\times 10^{-17} \text{ cm}^3 \text{ molecule}^{-1} \text{ s}^{-1}$ for 1P3OL and (16.90 ± 2.49) $\times 10^{-17}$
324 $\text{ cm}^3 \text{ molecule}^{-1} \text{ s}^{-1}$ for c-2P1OL at room temperature. More recently, O'Dwyer et al., (2010)
325 used the absolute method to determine an ozonolysis rate constant of (1.64 ± 0.15) $\times 10^{-17}$
326 $\text{ cm}^3 \text{ molecule}^{-1} \text{ s}^{-1}$ for 1P3OL and (11.50 ± 0.66) $\times 10^{-17} \text{ cm}^3 \text{ molecule}^{-1} \text{ s}^{-1}$ for c-2P1OL at
327 room temperature. For 1P3OL, the obtained average ambient rate constant is in a good
328 agreement with the available literature with a difference of about 6% with Grosjean and
329 Grosjean (1994) and 2% with O'Dwyer et al. (2010). In the case of c-2P1OL, ~38%
330 discrepancy is observed with Grosjean and Grosjean (1994). However, the rate constant
331 determined by O'Dwyer et al. (2010) at room temperature is in a very good agreement with
332 our average rate constant (~9%). Our determinations are closer to those of O'Dwyer et al.
333 (2010) and the observed difference lies in our uncertainties' domain.

334 Gibilisco et al., (2015b) determined an ozonolysis rate constant of t-3H1OL of ($5.83 \pm$
335 0.86) $\times 10^{-17} \text{ cm}^3 \text{ molecule}^{-1} \text{ s}^{-1}$ at room temperature using the relative method while Lin et al.,
336 (2016) determined a rate constant of (6.19 ± 0.72) $\times 10^{-17} \text{ cm}^3 \text{ molecule}^{-1} \text{ s}^{-1}$ at room
337 temperature using the absolute method. These two determinations are in good agreement
338 with the average room temperature rate constant determined in this study with a difference
339 of about 7% and <1%, respectively.

340 As can be seen in **Table 1**, the Structure-Activity Relationship calculations (SAR) for
341 the ozonolysis of 1P3OL, c-2P1OL and t-3H1OL, obtained by McGillen et al. (2011), are in
342 a good agreement with the obtained experimental rate constants. The calculated rate
343 coefficients were ($10^{-17} \text{ cm}^3 \text{ molecule}^{-1} \text{ s}^{-1}$): 1.79 for 1P3OL, 16.8 for c-2P1OL and 6.38 for
344 c-3H1OL.

345 **4.6. Structure effect**

346 Under atmospheric conditions ($T = 298 \text{ K}$ and $P = 760 \text{ Torr}$), the kinetics of the
347 ozonolysis of the three unsaturated alcohols appear to be relatively sensitive to their
348 structure. Indeed, both experimental and theoretical works show that the reactivity of O_3

349 with 1P3OL is lower than that with c-2P1OL and t-3H1OL (**Table 1**). Our results show that
350 the unsaturated alcohol whose double bond is mono-substituted (1P3OL) is less reactive
351 than the unsaturated alcohols with di-substituted olefinic bond (c-2P1OL) and (t-3H1OL). In
352 addition, the comparison of the ozonolysis rate constant of c-2P1OL with that of t-3H1OL
353 shows that the position of the OH-group impacts the ozonolysis kinetics.

354 In order to extract structure-reactivity trends, the experimental rate constants of the
355 reaction of ozone with 1P3OL, c-2P1OL and t-3H1OL were compared with those of other
356 C₃-C₆ unsaturated alcohols found in the literature (**Table 2**). From this table the following
357 points emerge:

- 358 • The kinetics of ozonolysis are mainly influenced by the substitution degree of the
359 double bond. It increases with the number of substituents. This finding is expected
360 since the ozonolysis reaction occurs by electrophilic addition of ozone to the double
361 bond. As a result, the reactivity should increase with the number of hydroxyalkyl
362 substituents.
- 363 • In the case of mono-substituted unsaturated alcohols, with the exception of 3-methyl-
364 1-buten-3-ol, the nature of the hydroxy alkyl substituent has no influence on the
365 ozonolysis kinetics.
- 366 • In the case of di-substituted C₄-C₆ unsaturated alcohols, the presence of an -OH group
367 in the beta position seems to enhance the rate constant more than in the gamma
368 position where the OH group is further from the double bond. So, 2-buten-1-ol and
369 cis-2-penten-1-ol with OH in β -position are more reactive than trans-3-hexen-1-ol and
370 cis-3-hexen-1-ol with OH in γ -position, with the exception of trans-2-hexen-1-ol
371 where its rate constant is of the same order of that of trans 3-hexen-1-ol. The SAR
372 calculation obtained by McGillen et al. (2011) also predicts a much faster rate constant
373 for c-2P1OL than for t-3H1OL.

374 In order to evaluate the effect of the hydroxyl group (-OH) on the reactivity of
375 unsaturated organic compounds, the kinetic results obtained in this study and previous
376 studies found in the literature are compared to those reported for their homologous alkenes
377 (**Table 2**). It is found that C₃-C₅ unsaturated alcohols with a mono-substituted C = C bond
378 are slightly more reactive than their homologous alkenes with the exception of 3-methyl-1-
379 buten-3-ol. This observation is unexpected because the presence of an hydroxyl group exerts
380 an attracting effect which can reduce the electronic density of the double bond deactivating
381 the ozone addition. However, the reactivity of C₄ -C₆ di-substituted alcohols is relatively

382 lower than that of their homologous alkene with the exception of 2-buten-1-ol. This can be
383 explained by the attraction effect of the hydroxyl group.

384 *4.7. Temperature effect*

385 Ozonolysis rate constants determined in this study show a low positive temperature
386 dependence. Taken into account uncertainties, activation energy E_a for the ozonolysis of the
387 three unsaturated alcohols are of the same order of magnitude. The position of the double
388 bond and the OH group do not have much impact on this parameter. On the other hand, the
389 pre-exponential factor A is sensitive to the position of the double bond: the more the olefinic
390 bond is substituted, the higher A is.

391 The kinetic parameters (E_a and A) determined in this work for unsaturated alcohols are
392 compared with those of their corresponding alkenes. Since the kinetic parameters (E_a and A)
393 are not available for trans-3-hexene, the homologous alkene of t-3H1OL, the comparison is
394 made with respect to trans-2-hexene (**Table 3**).

395 The ozonolysis activation energies of the unsaturated alcohols are slightly lower than
396 those of their homologous alkenes, except for 1-penten-3-ol, whose activation energy is
397 approximately two times lower. The pre-exponential factors for unsaturated alcohols are
398 slightly lower than those of their homologous alkenes.

399 *4.8. Atmospheric implications*

400 The experimental rate constants obtained in this work were used to estimate the
401 tropospheric lifetime of 1P3OL, c-2P1OL and t-3H1OL relative to ozone. To determine the
402 main chemical pathways for the atmospheric removal of these compounds, their
403 tropospheric lifetimes with respect to their reactions with OH, NO_3 and Cl radicals were
404 determined. Tropospheric lifetimes are calculated using the expression: $\tau_X = 1/k_X [X]$ where
405 $[X]$ is the average concentration of OH, Cl, NO_3 , and O_3 , and k_X the reactions rate constants
406 with the oxidant X. The tropospheric lifetime values for the studied alcohols are summarized
407 in **Table 4**.

408 A daily average global tropospheric concentration of 24 h of 1×10^6 molecules cm^{-3}
409 (Atkinson et al., 1995; Finlayson-Pitts and Pitts, 2000) was used to calculate tropospheric
410 lifetime due to OH-reaction, an average concentration of 10^{12} molecules cm^{-3} for ozone-
411 reaction (Finlayson-Pitts and Pitts, 2000; Vingarzan, 2004), 3×10^9 for nitrate -reaction
412 (Calvert et al., 2000) and 10^4 for chlorine atoms-reaction (Finlayson-Pitts and Pitts, 2000).

413 According to **Table 4**, it can be deduced that unsaturated alcohols are very reactive
414 with respect to their reaction with OH, NO₃ and O₃ with tropospheric lifetimes of few
415 minutes (13-36 min) to few hours (2-17h). Thus, their actual lifetimes depend mainly on the
416 local chemical composition and the location of their emission sources. The calculated
417 lifetimes can provide an order of magnitude of this parameter and get an idea of their
418 atmospheric persistence.

419 **5. Conclusion**

420 The first temperature dependent rate constants for the reaction of the three unsaturated
421 alcohols (1-penten-3-ol, cis-2-penten-1-ol and trans-3-hexen-1-ol) with ozone O₃ were
422 determined using the relative method, in a pyrex reactor coupled to a FTIR spectrometer and
423 to a GC/MS. The kinetic results showed a low positive temperature dependence over the
424 temperature range 273-333 K. Activation energies E_a are of the same order of magnitude
425 considering uncertainties. In fact, the position of the double bond and the OH group does not
426 have much impact on this parameter. However, the pre-exponential factor A is sensitive to
427 the position of the double bond.

428 The studied reactions were also explored theoretically for the first time using
429 computational methods based on quantum chemical theory characterizing the intermediates,
430 transition states and the subsequent formation of reaction products. The rate constants were
431 calculated at room temperature employing modified transition-state theory (MTST). The rate
432 constants obtained theoretically were found to be lower than those obtained experimentally
433 but remain in the same order of magnitude.

434 Both experimental and theoretical works show that the rate constants for the reaction
435 of unsaturated alcohols with ozone increase from a mono-substituted unsaturated alcohol to
436 a di-substituted unsaturated alcohol. Unsaturated alcohols are very reactive with atmospheric
437 lifetimes varying from few minutes with nitrate radicals to few hours with OH and O₃.

438 **Acknowledgment**

439 The authors are very grateful to the INSU-LEFE CHAT program for the financial support.
440 Thanks are also due to the Head, Department of Chemistry, DDU Gorakhpur University for
441 availing the computational facilities and to UGC for financial support to PKR under its
442 startup grant.

443

444

445 **References**

446 Al Rashidi, M., El Masri, A., Roth, E., Chakir, A., 2014. UV spectra and OH-oxidation
447 kinetics of gaseous phase morpholinic compounds. *Atmos. Environ.* 88, 261–268.
448 <https://doi.org/10.1016/j.atmosenv.2014.01.057>

449 Atkinson, R., Arey, J., Aschmann, S.M., Corchnoy, S.B., Shu, Y., 1995. Rate constants for
450 the gas-phase reactions of cis-3-hexen-1-ol, cis-3-hexenylacetate, trans-2-hexenal, and
451 linalool with OH and NO₃ radicals and O₃ at 296, and OH radical formation yields from
452 the O₃ reactions. *Int. J. Chem. Kinet.* 27, 941–955. [https://doi.org/10.1002/kin.](https://doi.org/10.1002/kin.550271002)
453 550271002

454 Avzianova, E.V., Ariya, P.A., 2002. Temperature-dependent kinetic study for ozonolysis of
455 selected tropospheric alkenes. *Int. J. Chem. Kinet.* 34, 678–684. [https://doi.org/](https://doi.org/10.1002/kin.10093)
456 10.1002/kin.10093

457 Calvert, J.G., Atkinson, R., Kerr, J.A., Madronich, S., Moortgat, G.K., Wallington, T.J.,
458 Yarwood, G., 2000. *The mechanisms of atmospheric oxidation of the alkenes*. Oxford
459 University Press, 2000, New York

460 Davis, M.E., Burkholder, J.B., 2011. Rate coefficients for the gas-phase reaction of OH with
461 (Z)-3-hexen-1-ol, 1-penten-3-ol, (E)-2-penten-1-ol, and (E)-2-hexen-1-ol between 243
462 and 404K. *Atmos. Chem. Phys.* 11, 3347–3358. [https://doi.org/10.5194/acp-11-3347](https://doi.org/10.5194/acp-11-3347-2011)
463 2011

464 Davis, M.E., Gilles, M.K., Ravishankara, A.R., Burkholder, J.B., 2007. Rate coefficients for
465 the reaction of OH with (E)-2-pentenal, (E)-2-hexenal, and (E)-2-heptenal. *Phys. Chem.*
466 *Chem. Phys.* 9, 2240-8. <https://doi.org/10.1039/b700235>

467 Finlayson-Pitts, B.J., Pitts (Jr.), James, N.J., 2000. *Chemistry of the Upper and Lower*
468 *Atmosphere: Theory, Experiments, and Applications*. Academic Press, New York

469 Fisher, A.J., Grimes, H.D., Fall, R., 2003. The biochemical origin of pentenol emissions
470 from wounded leaves. *Phytochemistry* 62, 159–163. [https://doi.org/10.1016/S0031-](https://doi.org/10.1016/S0031-9422(02)00521-6)
471 9422(02)00521-6

472 Frisch, M.J., Trucks, G.W., Schlegel, H.B., Scuseria, G.E., Robb, M.A., Cheeseman, J.R.,
473 Montgomery, J.A., Vreven Jr, T., Kudin, K.N., Burant, J.C., 2008. Gaussian 09,

- 474 revision B. 01, Gaussian, Inc., Wallingford, CT, 2009 Search PubMed;(b) NM O'Boyle,
475 AL Tenderholt and KM Langner. *J. Comput. Chem* 29, 839.
- 476 Fuentes, J.D., Lerdau, M., Atkinson, R., Baldocchi, D., Bottenheim, J.W., Ciccioli, P.,
477 Lamb, B., Geron, C., Gu, L., Guenther, A., Sharkey, T.D., Stockwell, W., 2000.
478 Biogenic Hydrocarbons in the Atmospheric Boundary Layer: A Review. *Bull. Am.*
479 *Meteorol. Soc.* 81, 1537–1575. [https://doi.org/10.1175/1520-0477\(2000\)081<1537:](https://doi.org/10.1175/1520-0477(2000)081<1537:)
480 [BHITAB>2.3.CO;25](https://doi.org/10.1175/1520-0477(2000)081<1537:)
- 481 Gadzhiev, O.B., Ignatov, S.K., Krisyuk, B.E., Maierov, A.V., Gangopadhyay, S., Masunov,
482 A.E., 2012. Quantum chemical study of the primary step of ozone addition at the double
483 bond of ethylene. *J. Phys. Chem. A* 116, 10420–10434. <https://doi.org/10.1134/>
484 [s0023158411060103](https://doi.org/10.1134/s0023158411060103)
- 485 Gibilisco, R.G., Bejan, I., Barnes, I., Wiesen, P., Teruel, M.A., 2015a. FTIR gas kinetic
486 study of the reactions of ozone with a series of hexenols at atmospheric pressure and
487 298 K. *Chem. Phys. Lett.* 618, 114–118. <https://doi.org/10.1016/j.cplett.2014.11.003>
- 488 Gibilisco, R.G., Bejan, I., Barnes, I., Wiesen, P., Teruel, M.A., 2014. Rate coefficients at
489 298K and 1atm for the tropospheric degradation of a series of C6, C7 and C8 biogenic
490 unsaturated alcohols initiated by Cl atoms. *Atmos. Environ.* 94, 564–572.
491 <https://doi.org/10.1016/j.atmosenv.2014.05.050>
- 492 Gibilisco, R.G., Blanco, M.B., Bejan, I., Barnes, I., Wiesen, P., Teruel, M.A., 2015b.
493 Atmospheric Sink of (E)-3-Hexen-1-ol, (Z)-3-Hepten-1-ol, and (Z)-3-Octen-1-ol:
494 Rate Coefficients and Mechanisms of the OH-Radical Initiated Degradation. *Environ.*
495 *Sci. Technol.* 49, 7717–7725. <https://doi.org/10.1021/es506125c>
- 496 Gibilisco, R.G., Santiago, A.N., Teruel, M.A., 2013. OH-initiated degradation of a series of
497 hexenols in the troposphere. Rate coefficients at 298K and 1atm. *Atmos. Environ.* 77,
498 358–364. <https://doi.org/10.1016/j.atmosenv.2013.05.019>
- 499 Gonzalez, C., Schlegel, B.H., 1989. An improved algorithm for reaction path following. *J.*
500 *Chem. Phys.* 90, 2154–2161. <https://doi.org/10.1063/1.456010>
- 501 Grosjean, E., Grosjean, D., Williams II, E.L., 1993. Rate constants for the gas-phase
502 reactions of ozone with unsaturated alcohols, esters, and carbonyls. *Int. J. Chem. Kinet.*
503 25, 783–794. <https://doi.org/10.1002/kin.550250909>

- 504 Grosjean, E., Grosjean, D., 1994. Rate Constants for the gas-phase reactions of Ozone with
505 unsaturated Aliphatic Alcohols. *Int. J. Chem. Kinet.* 26, 1185–1191. [https://doi.org](https://doi.org/10.1002/kin.550261206)
506 [/https://doi.org/10.1002/kin.550261206](https://doi.org/10.1002/kin.550261206)
- 507 Grosjean, E., Grosjean, D., 1995. Rate constants for the gas-phase reaction of C₅ - C₁₀
508 alkenes with ozone, *Int J. Chem. Kinet.* 27, 1045-1054, [https://doi.org/10.1002/](https://doi.org/10.1002/kin.550271102)
509 [kin.550271102](https://doi.org/10.1002/kin.550271102)
- 510 Grosjean, E., Grosjean, D., 1996. Rate constants for the gas-phase reaction of ozone with
511 1,2-disubstituted alkenes, 28, 441-466, [http:// doi.org/10.1002/\(SISI\)/1097-4601\(1996\)](http://doi.org/10.1002/(SISI)/1097-4601(1996)28:6<461::AID-KIN8>3.0.CO;2-T)
512 [28:6<461::AID-KIN8>3.0.CO:2-T](http://doi.org/10.1002/(SISI)/1097-4601(1996)28:6<461::AID-KIN8>3.0.CO;2-T).
- 513 James, W.H., Buchanan, E.G., Müller, C.W., Dean, J.C., Kosenkov, D., Slipchenko, L.V.,
514 Guo, L., Reidenbach, A.G., Gellman, S.H., Zwier, T.S., 2011. Evolution of amide
515 stacking in larger γ -peptides: Triamide H-bonded cycles. *J. Phys. Chem. A* 115, 13783–
516 13798. <https://doi.org/10.1021/jp205527e>
- 517 Heiden, A.C., Kobel, K., Langebartels, C., Schuh-Thomas, G., Wildt, J., 2003. Emissions of
518 oxygenated volatile organic compounds from plants part I: Emissions from
519 lipoxygenase activity. *J. Atmos. Chem.* 45, 143–172. [https://doi.org/10.1023/](https://doi.org/10.1023/A:1024069605420)
520 [A:1024069605420](https://doi.org/10.1023/A:1024069605420)
- 521 Kalalian, C., Roth, E., Chakir, A., 2017. Rate Coefficients for the Gas-Phase Reaction of
522 Ozone with C₅ and C₆ Unsaturated Aldehydes. *Int. J. Chem. Kinet.* 50, 47–56. [https://](https://doi.org/10.1002/kin.21139)
523 doi.org/10.1002/kin.21139
- 524 Karl, T., Fall, R., Jordan, A., Lindinger, W., 2001. On-line analysis of reactive VOCs from
525 urban lawn mowing. *Environ. Sci. Technol.* 35, 2926–2931. [https://doi.org/10.1021/](https://doi.org/10.1021/es010637y)
526 [es010637y](https://doi.org/10.1021/es010637y)
- 527 Kirstine, W., Galbally, I., Ye, Y., Hooper, M., 1998. Emissions of volatile organic
528 compounds (primarily oxygenated species) from pasture. *J. Geophys. Res.* 103,
529 10605–10619. [https://doi.org/https://doi.org/10.1029/97JD03753](https://doi.org/10.1029/97JD03753)
- 530 Klawatsch-Carrasco, N., Doussin, J.F., Carlier, P., 2004. Absolute rate constants for the gas-
531 phase ozonolysis of isoprene and methylbutenol. *Int. J. Chem. Kinet.* 36, 152–156.
532 <https://doi.org/10.1002/kin.10175>
- 533 Krasnoperov, L.N., Peng, J., Marshall, P., 2006. Modified transition state theory and

- 534 negative apparent activation energies of simple metathesis reactions: Application to the
535 reaction $\text{CH}_3 + \text{HBr} \rightarrow \text{CH}_4 + \text{Br}$. *J. Phys. Chem. A* 110, 3110–3120. [https://doi.org/](https://doi.org/10.1021/jp054435q)
536 10.1021/jp054435q
- 537 Laversin, H., El Masri, A., Al Rashidi, M., Roth, E., Chakir, A., 2016. Kinetic of the gas-
538 phase reactions of OH radicals and Cl atoms with diethyl ethylphosphonate and triethyl
539 phosphate. *Atmos. Environ.* 126, 250–257. [https://doi.org/10.1016/j.atmosenv.](https://doi.org/10.1016/j.atmosenv.2015.11.057)
540 2015.11.057
- 541 Le Calvé, S., Mellouki, A., Le Bras, G., Treacy, J., Wenger, J., Sidebottom, H., 2000.
542 Kinetic studies of OH and O₃ reactions with allyl and isopropenyl acetate. *J. Atmos.*
543 *Chem.* 37, 161–172. <https://doi.org/10.1023/A:1006499008759>
- 544 Li, G., Li, Q.S., Xie, Y., Schaefer, H.F., 2015. From Gas-Phase to Liquid-Water Chemical
545 Reactions: The Fluorine Atom Plus Water Trimer System. *Angew. Chemie - Int. Ed.* 54,
546 11223–11226. <https://doi.org/10.1002/anie.201505075>
- 547 Lin, X., Ma, Q., Yang, C., Tang, X., Zhao, W., Hu, C., Gu, X., Fang, B., Gai, Y., Zhang, W.,
548 2016. Kinetics and mechanisms of gas phase reactions of hexenols with ozone. *RSC*
549 *Adv.* 6, 83573–83580. <https://doi.org/10.1039/C6RA17107A>
- 550 McGillen, M.R., Archibald, A.T., Carey, T., Leather, K.E., Shallcross, D.E., Wenger, J.C.,
551 Percival, C.J., 2011. Structure-activity relationship (SAR) for the prediction of gas-
552 phase ozonolysis rate coefficients: an extension towards heteroatomic unsaturated
553 species. *Phys. Chem. Chem. Phys.* 13, 2842–2849. [https://doi.org/10.1039/C0CP](https://doi.org/10.1039/C0CP01732A)
554 01732A
- 555 Mellouki, A., Le Bras, G., Sidebottom, H., 2003. Kinetics and Mechanisms of the Oxidation
556 of Oxygenated Organic Compounds in the Gas Phase. *Chem. Rev.* 103, 5077–5096.
557 <https://doi.org/10.1021/cr020526x>
- 558 Messaadia, L., El Dib, G., Lendar, M., Cazaunau, M., Roth, E., Ferhati, A., Mellouki, A.,
559 Chakir, A., 2013. Gas-phase rate coefficients for the reaction of 3-hydroxy-2-butanone
560 and 4-hydroxy-2-butanone with OH and Cl. *Atmos. Environ.* 77, 951–958. [https://](https://doi.org/10.1016/j.atmosenv.2013.06.028)
561 doi.org/10.1016/j.atmosenv.2013.06.028
- 562 O'Dwyer, M.A., Carey, T.J., Healy, R.M., Wenger, J.C., Picquet-Varrault, B., Doussin, J.F.,
563 2010. The gas-phase ozonolysis of 1-penten-3-ol, (Z)-2-penten-1-ol and 1-penten-3-
564 one: Kinetics, products and secondary organic aerosol Formation. *Zeitschrift fur Phys.*

- 565 Chemie 224, 1059–1080. <https://doi.org/10.1524/zpch.2010.6141>
- 566 Olzmann, M., Kraka, E., Cremer, D., Gutbrod, R., Andersson, S., 1997. Energetics, kinetics,
567 and product distributions of the reactions of ozone with ethene and 2,3-dimethyl-2-
568 butene. *J. Phys. Chem. A* 101, 9421–9429. <https://doi.org/10.1021/jp971663e>
- 569 Orlando, J.J., Tyndall, G.S., Ceazan, N., 2001. Rate Coefficients and Product Yields from
570 Reaction of OH with 1-Penten-3-ol, (Z)-2-Penten-1-ol, and Allyl Alcohol (2-Propen-1-
571 ol). *J. Phys. Chem. A* 105, 3564–3569. <https://doi.org/10.1021/jp0041712>
- 572 Papagni, C., Arey, J., Atkinson, R., 2009. Rate Constants for the Gas-Phase Reactions of
573 OH Radicals with a Series of Unsaturated Alcohols. *J. Phys. Chem. A* 113, 852–857.
574 [https://doi.org/https://doi.org/10.1002/1097-4601\(200102\)33:2<142::AID-
575 KIN1007>3.0.CO;2-F](https://doi.org/10.1002/1097-4601(200102)33:2<142::AID-KIN1007>3.0.CO;2-F)
- 576 Parker, J.K., Espada-Jallad, C., 2009. Kinetics of the Gas-Phase Reactions of OH and NO₃
577 Radicals and O₃ with Allyl Alcohol and Allyl Isocyanate. *J. Phys. Chem. A* 113, 9814–
578 9824. <https://doi.org/10.1021/jp9055939>
- 579 Pfrang, C., Baeza Romero, M.T., Cabanas, B., Canosa-Mas, C.E., Villanueva, F., Wayne,
580 R.P., 2007. Night-time tropospheric chemistry of the unsaturated alcohols (Z)-pent-2-
581 en-1-ol and pent-1-en-3-ol: Kinetic studies of reactions of NO₃ and N₂O₅ with stress-
582 induced plant emissions. *Atmos. Environ.* 41, 1652–1662. [https://doi.org/10.1016/
583 j.atmosenv.2006.10.034](https://doi.org/10.1016/j.atmosenv.2006.10.034)
- 584 Pfrang, C., Martin, R.S., Canosa-Mas, C.E., Wayne, R.P., 2006. Gas-phase reactions of NO₃
585 and N₂O₅ with (Z)-hex-4-en-1-ol, (Z)-hex-3-en-1-ol ('leaf alcohol'), (E)-hex-3-en-1-
586 ol, (Z)-hex-2-en-1-ol and (E)-hex-2-en-1-ol. *Phys. Chem. Chem. Phys.* 8, 354–363.
587 <https://doi.org/10.1039/B510835G>
- 588 Rao, P.K., Gejji, S.P., 2018. Atmospheric degradation of HCFO-1233zd(E) initiated by OH
589 radical, Cl atom and O₃ molecule: Kinetics, reaction mechanisms and implications. *J.*
590 *Fluor. Chem.* 211, 180–193. <https://doi.org/10.1016/j.jfluchem.2018.05.001>
- 591 Rao, P.K., Gejji, S.P., 2017a. Molecular insights for the HFO-1345fz + X (X = Cl, O₃ or
592 NO₃[rad]) reaction and fate of alkoxy radicals initiated by Cl: DFT investigations. *J.*
593 *Fluor. Chem.* 204, 65–75. <https://doi.org/10.1016/j.jfluchem.2017.08.015>
- 594 Rao, P.K., Gejji, S.P., 2017b. Kinetics and mechanistic investigations of atmospheric

- 595 oxidation of HFO-1345fz by OH radical: Insights from theory. *J. Phys. Chem. A* 121,
596 595–607. <https://doi.org/10.1021/acs.jpca.6b11312>
- 597 Rodríguez, A., Rodríguez, D., Garzón, A., Soto, A., Aranda, A., Notario, A., 2010. Kinetics
598 and mechanism of the atmospheric reactions of atomic chlorine with 1-penten-3-ol and
599 (Z)-2-penten-1-ol: an experimental and theoretical study. *Phys. Chem. Chem. Phys.* 12,
600 12245–12258. <https://doi.org/10.1039/c0cp00625d>
- 601 Vingarzan, R., 2004. A review of surface ozone background levels and trends. *Atmos.*
602 *Environ.* 38, 3431–3442. <https://doi.org/10.1016/j.atmosenv.2004.03.030>
- 603 Wegener, R., Brauers, T., Koppmann, R., Bares, S.R., Rohrer, F., Tillman, R., Wahner, A.,
604 Hansel, A., Wisthaler, A., 2007. Simulation chamber investigation of the reactions of
605 ozone with short-chained alkenes. *J. Geophys. Res. Atmos.* 112, 1–17. <https://doi.org/10.1029/2006JD007531>
- 607 Wigner, E., 1932. On the quantum correction for thermodynamic equilibrium. *Phys. Rev.*
608 40, 749–759. <https://doi.org/10.1103/PhysRev.40.749>
- 609 Xie, H. Bin, Ma, F., Wang, Y., He, N., Yu, Q., Chen, J., 2015. Quantum Chemical Study on
610 ·Cl-Initiated Atmospheric Degradation of Monoethanolamine. *Environ. Sci. Technol.*
611 49, 13246–13255. <https://doi.org/10.1021/acs.est.5b03324>
- 612 Zhang, D., Zhang, R., 2002. Mechanism of OH formation from ozonolysis of isoprene: A
613 quantum-chemical study. *J. Am. Chem. Soc.* 124, 2692–2703. [https://doi.org/10.1021/
614 ja011518l](https://doi.org/10.1021/ja011518l)
- 615 Zhao, Y., Truhlar, D.G., 2008. ChemInform Abstract: Density Functionals with Broad
616 Applicability in Chemistry. *ChemInform* 39, 157–167. [https://doi.org/10.1002/chin.
617 200821274](https://doi.org/10.1002/chin.200821274)
- 618 Zhao, Y., Truhlar, D.G., 2006. A new local density functional for main-group thermo-
619 chemistry, transition metal bonding, thermochemical kinetics, and noncovalent
620 interactions. *J. Chem. Phys.* 125. <https://doi.org/10.1063/1.2370993>
- 621

Table 1: Rate constants of the ozonolysis of 1P3OL, c-2P1OL and t-3H1OL at different temperatures obtained experimentally by FTIR and SPME-GC / MS and theoretically using M06-2X/6-311+G(d,p) method.

Compounds	FTIR			SPME-GC/MS		Theoretical calculation	Literature
	T (K)	R=k _{O3} /k _{ref} *	k _{O3} (x10 ¹⁷)**	R=k _{O3} /k _{ref} *	k _{O3} (x10 ¹⁷)**	k _{O3} (x10 ¹⁷)	k _{O3} (x10 ¹⁷)
1P3OL	273±2	0.81±0.04	1.24±0.24				-
	298±2	0.63±0.04	1.61±0.21	1.52±0.20	1.75±0.25	0.20	1.79±0.18 ^a
							1.64±0.15 ^b
							1.79 ^c
	313±2	0.50±0.12	1.67±0.43				-
333±2	0.51±0.06	2.04±0.28				-	
c-2P1OL	273±2	5.32±0.10	8.09±1.55				-
	298±2	4.68±0.15	11.90±1.41	5.40±0.20	9.07±1.29	1.48	16.90±2.49 ^a
							11.50±0.66 ^b
							16.80 ^c
	313±2	3.77±0.28	12.50±1.44				-
333±2	3.86±0.03	15.40±1.13				-	
t-3H1OL	273±2	2.71±0.20	4.12±0.84				-
	298±2	2.35±0.28	5.97±0.99	3.90±0.20	6.50±0.95	1.50	5.83±0.86 ^d
							6.19±0.72 ^e
							6.38 ^c
	313±2	1.87±0.26	6.21±1.02				-
333±2	2.05±0.08	8.20±0.68				-	

a : (Grosjean and Grosjean. 1993) ; b : (O'Dwyer et al.. 2010) ; c: SAR calculations by (McGillen et al., 2011); d : (Gibilisco et al., 2015b) ; e:(Lin et al.. 2016).

* : error= 2σ ; ** : uncertainties calculated by the error propagation method

Table 2: Comparison of the reactivity of C₃-C₆ unsaturated alcohols with ozone

ROH	k_{O_3} ($\times 10^{17}$ $\text{cm}^3 \text{molecule}^{-1} \text{s}^{-1}$)	Homologous alkenes	k_{O_3} ($\times 10^{17}$ $\text{cm}^3 \text{molecule}^{-1} \text{s}^{-1}$)
mono-substituted alcohol			
1-Propen-3-ol CH₂=CHCH₂OH	1.63±0.03 ^a	Propene ^h	1.06±0.12
1-Buten-3-ol CH₂=CHCH(OH)CH₃	1.63±0.06 ^b	1-butene ^h	0.96±0.09
1-Penten-3-ol* CH₂=CHCH(OH)CH₂CH₃	1.68±0.32 ^c	1-pentene ⁱ	1.00±0.01
3-Methyl-1-buten-3-ol CH₂=CHC(OH)(CH₃)₂	0.83±0.10 ^d	3-methyl-1- butene ^j	0.95±0.12
di-substituted alcohol			
2-Buten-1-ol CH₃CH=CHCH₂OH	25.00±4.00 ^b	Cis-2-butene ^h	12.90±1.13
Cis-2-penten-1-ol * CH₃CH₂CH=CHCH₂OH	10.50±1.99 ^c	Cis-2-pentene ⁱ	12.82±0.45
Cis-3-hexen-1-ol CH₃CH₂CH=CH₂CH₂CH₂OH	6.39±1.66 ^e 10.50±0.70 ^f	Cis-3-hexene ^j	14.40±1.66
Trans-3-hexen-1-ol * CH₃CH₂CH=CH₂CH₂CH₂OH	6.24±1.37	Trans-3- hexene ^j	15.70±2.49
Trans-2-hexen-1-ol CH₃CH₂CH₂CH=CHCH₂OH	5.98±0.73 ^g	Trans-2- hexene ⁱ	21.50±0.54

a: (Parker and Espada-Jallad, 2009), b:(Grosjean and Grosjean, 1994); c : This work, average of the two determinations by FTIR and SPME-GC/MS ; d : (Klawatsch-Carrasco et al., 2004) ; e : (Atkinson et al., 1995) ; f : (Grosjean and Grosjean, 1994) ; g :(Gibilisco et al., 2015a) h :(Wegener et al., 2007) ; i : (Avzianova and Ariya, 2002) ; j:(Grosjean and Grosjean, 1996)

*: average room temperature rate constant obtained by FTIR and GC/MS, uncertainty on this value was calculated using the error propagation method.

Table 1: Comparison of activation energies E_a and pre-exponential factors A of 1P3OL, c-2P1OL and t-3H1OL with their homologous alkenes.

Compounds	Activation energy E_a (J/mol)	$A \times 10^{16}$ (cm ³ molecule ⁻¹ s ⁻¹)	Homologous alkenes	Activation energy E_a (J/mol)	$A \times 10^{15}$ (cm ³ molecule ⁻¹ s ⁻¹)
1P3OL	6054 ± 2398	1.80 ± 1.67	1-pentene ^a	13 125 ± 669	1.70±0.10
c-2P1OL	7501 ± 2179	23. 10 ± 19.26	Cis-2-pentene ^a	8 326 ± 293	3.70±0.17
t-3H1OL	8436 ± 2269	17.10 ± 14.74	Trans-2-hexene ^a	9672±222	7.60±0.18

a : (Avzianova and Ariya, 2002)

Table Error! No text of specified style in document.: Tropospheric lifetimes of 1P3OL, c-2P1OL and t-3H1OL with OH, O₃, NO₃ and Cl

Compounds	$\tau_{\text{OH}}^{\text{a}}$	$\tau_{\text{O}_3}^{\text{b}}$	$\tau_{\text{NO}_3}^{\text{c}}$	$\tau_{\text{Cl}}^{\text{d}}$
1P3OL	4 h	17 h	7h	5 d
c-2P1OL	3 h	3 h	36 min	4 d
t-3H1OL	2 h	4 h	13min	3d

[OH] = 1×10^6 molecules cm^{-3} (average overall tropospheric concentration during 24h), [O₃] = 10^{12} molecules cm^{-3} , [NO₃] = 3×10^9 and [Cl] = 10^4 molecules cm^{-3} .

a : k (OH + 1-penten-3-ol) and k (OH+cis-2-penten-1-ol) from Orlando et al. (2001); k (OH+ trans-3-hexen-1-ol) from Gibilisco et al. (2015).

b : this work

c : k (NO₃ + 1-penten-3-ol) and k (NO₃ + cis-2-penten-1-ol) from Pfrang et al. (2007) ; k (NO₃ + trans-3-hexen-1-ol) from Pfrang et al. (2006).

d : k (Cl + 1-penten-3-ol) and k (Cl + cis-2-penten-1-ol) from Rodríguez et al. (2010); k (Cl + trans-3-hexen-1-ol) from Gibilisco et al. (2014).

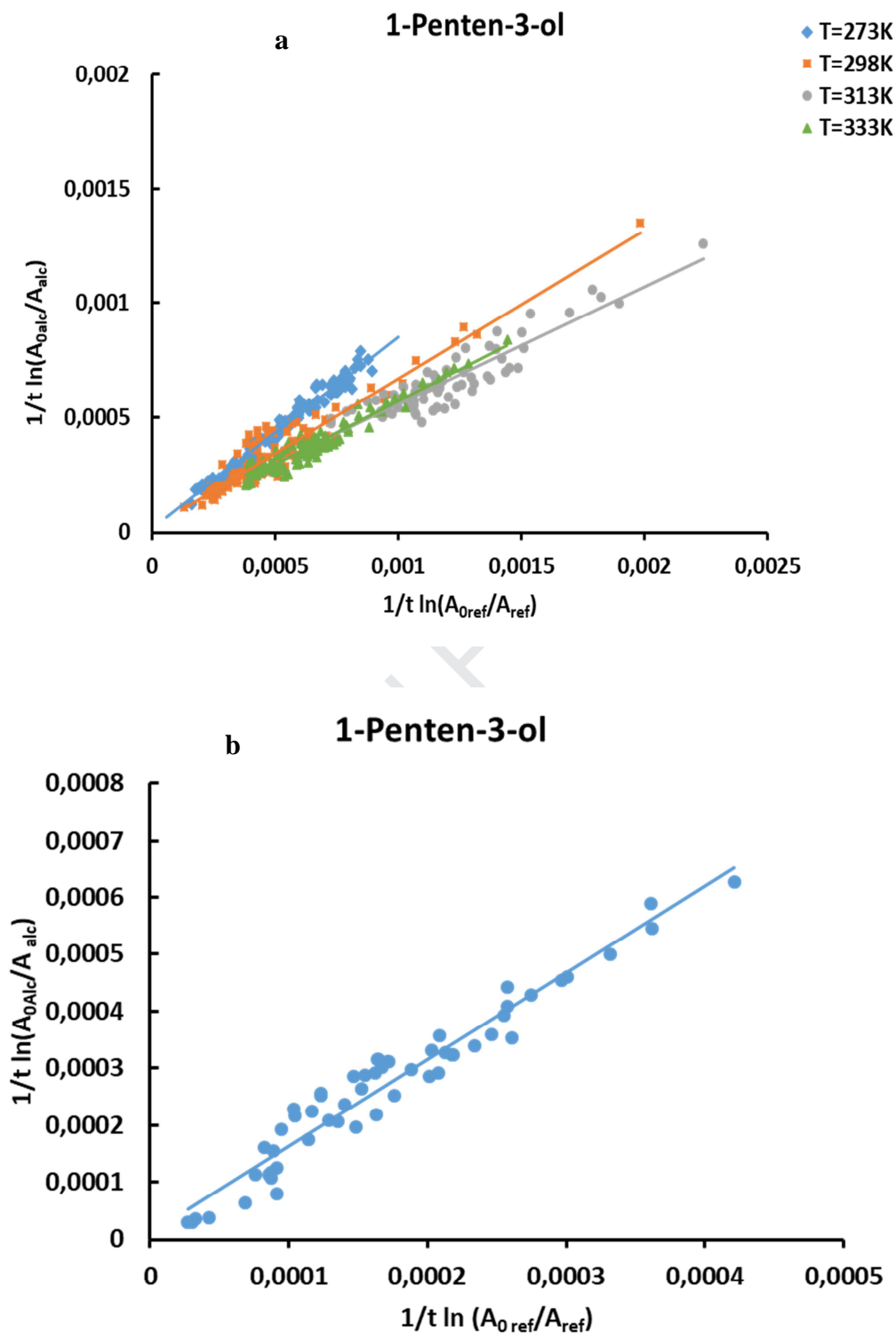


Fig. 1: Plot of $1/t \ln(A_{0alc}/A_{alc})$ vs $1/t \ln(A_{0ref}/A_{ref})$ for the ozonolysis of 1P3OL at 273, 298, 313 and 333K obtained by FTIR (a) and at $T = 298\text{K}$ by SPME -GC / MS (reference: 1-heptene) (b).

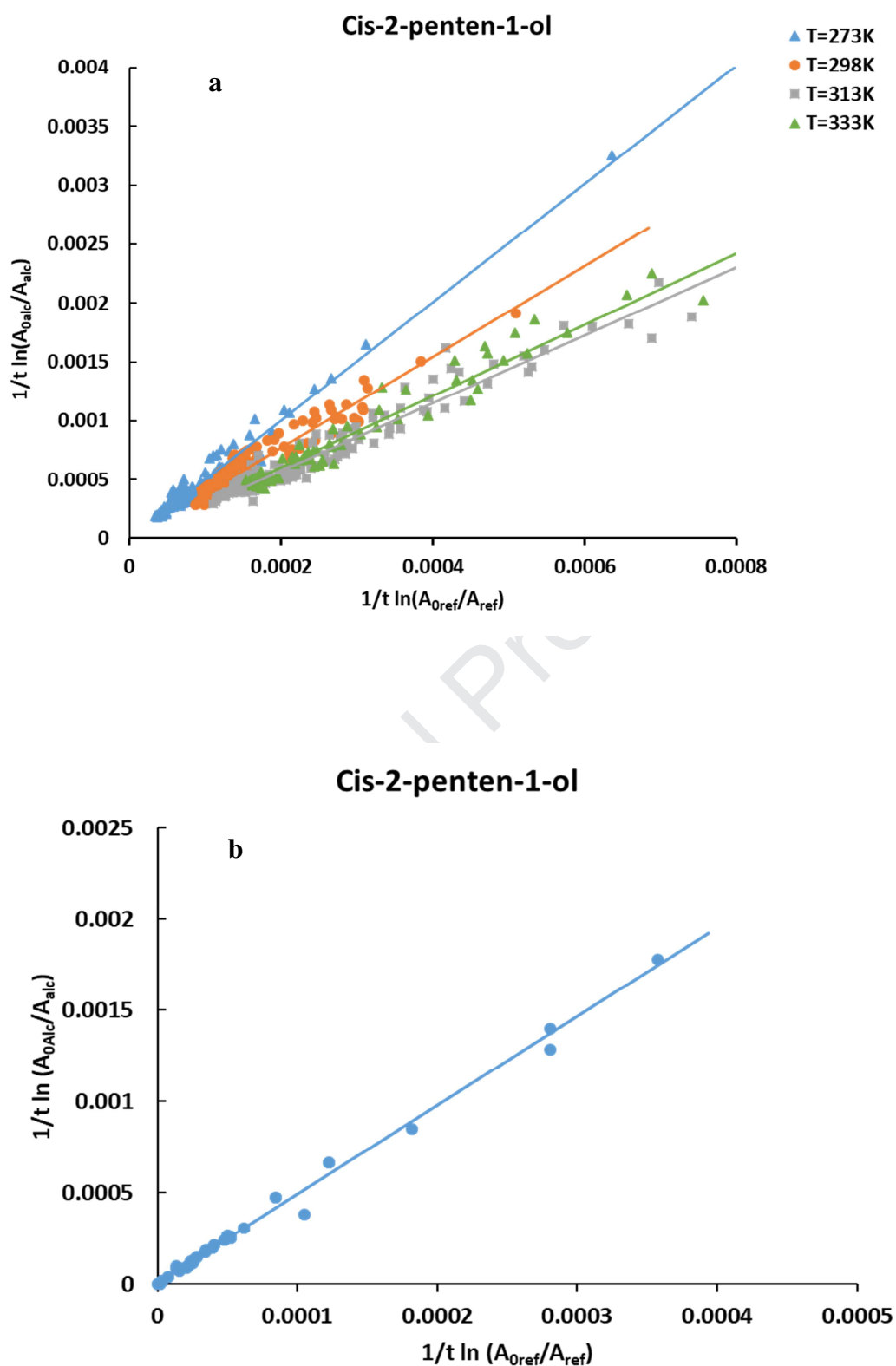


Fig. 2: Plot of $1/t \ln(A_{0alc}/A_{alc})$ vs $1/t \ln(A_{0ref}/A_{ref})$ for the ozonolysis of c-2P1OL at 273, 298, 313 and 333K obtained by FTIR (a) and at $T = 298\text{K}$ by SPME -GC / MS (reference: 1-penten-3-ol) (b).

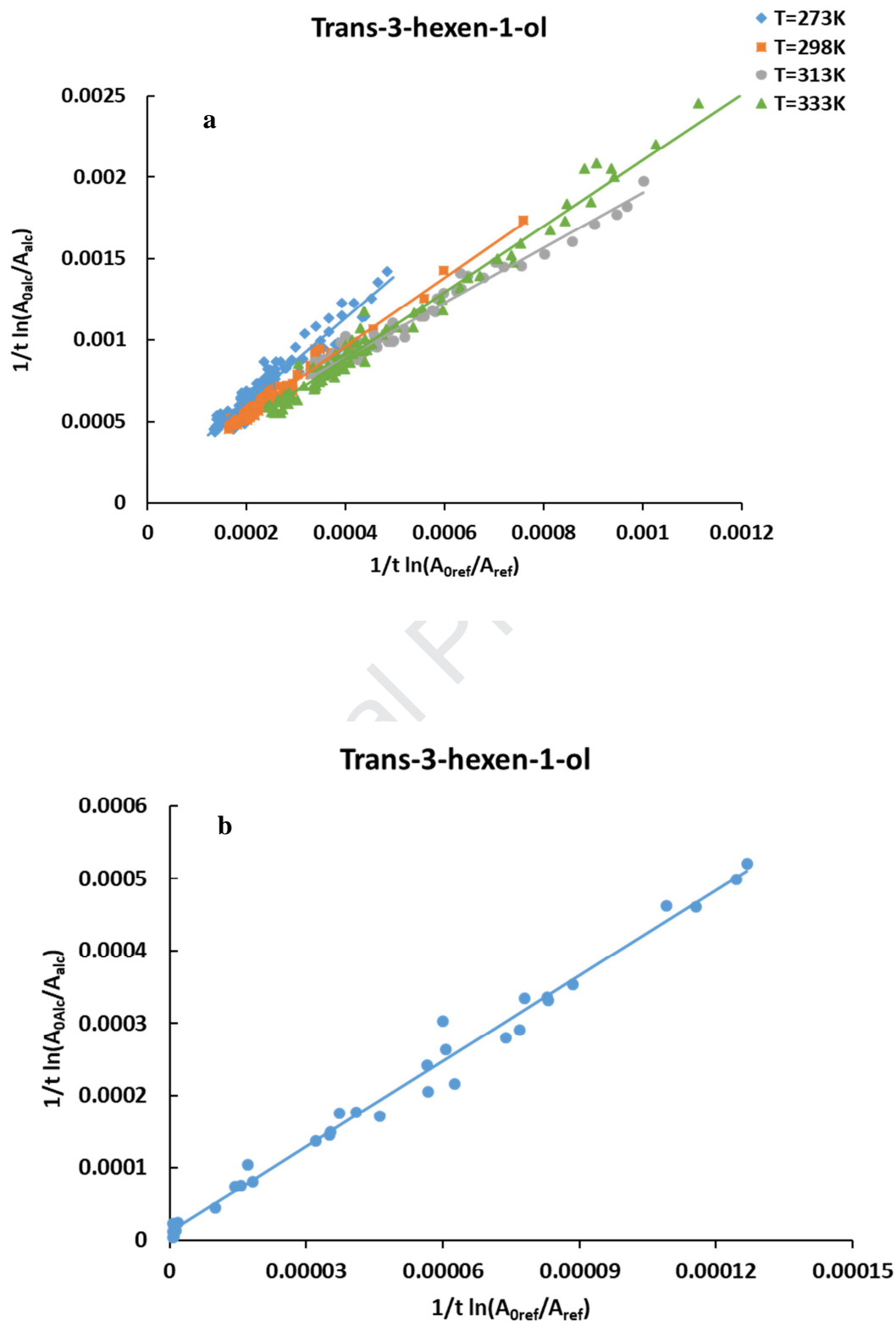


Fig. 3: Plot of $1/t \ln(A_{0alc}/A_{alc})$ vs $1/t \ln(A_{0ref}/A_{ref})$ for the ozonolysis of t-3H1OL at 273, 298, 313 and 333K obtained by FTIR (a) and at T = 298K by SPME -GC / MS (reference: 1-penten-3-ol) (b).

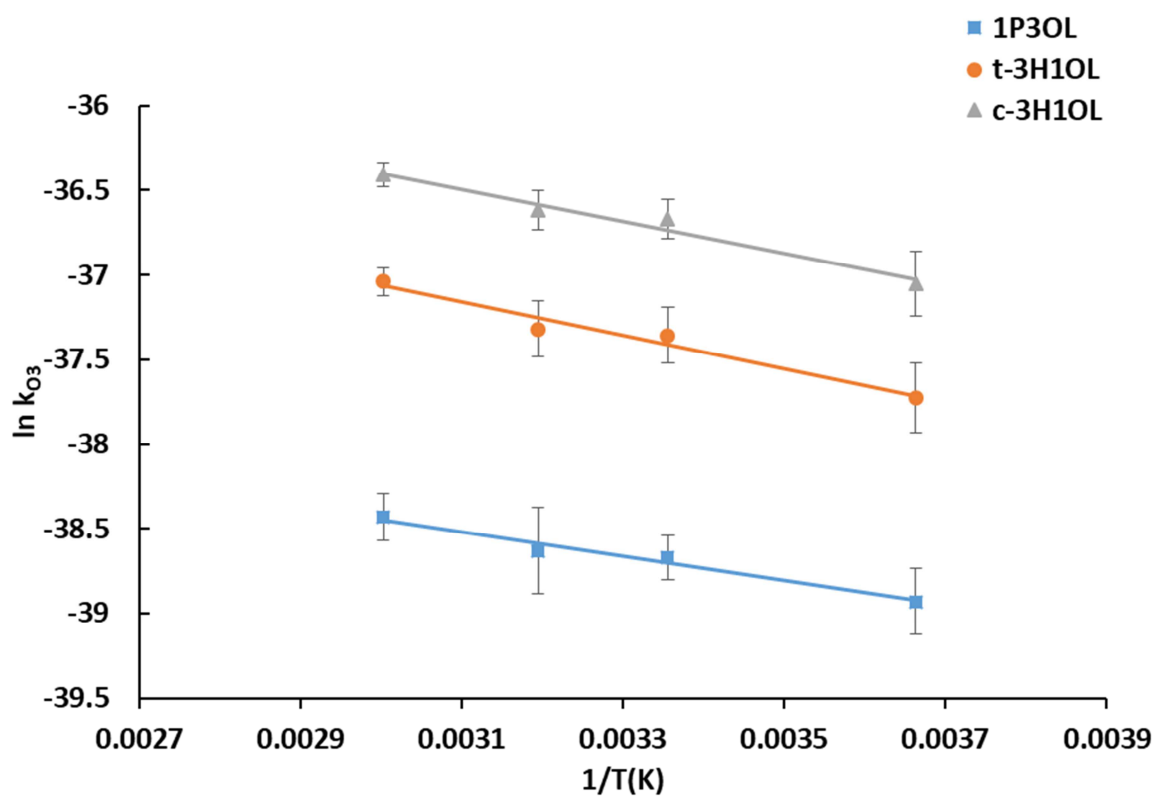


Fig. 4: Plot of $\ln k_{O_3}$ vs $1/T$ for 1P3OL, c-2P1OL and t-3H1OL.

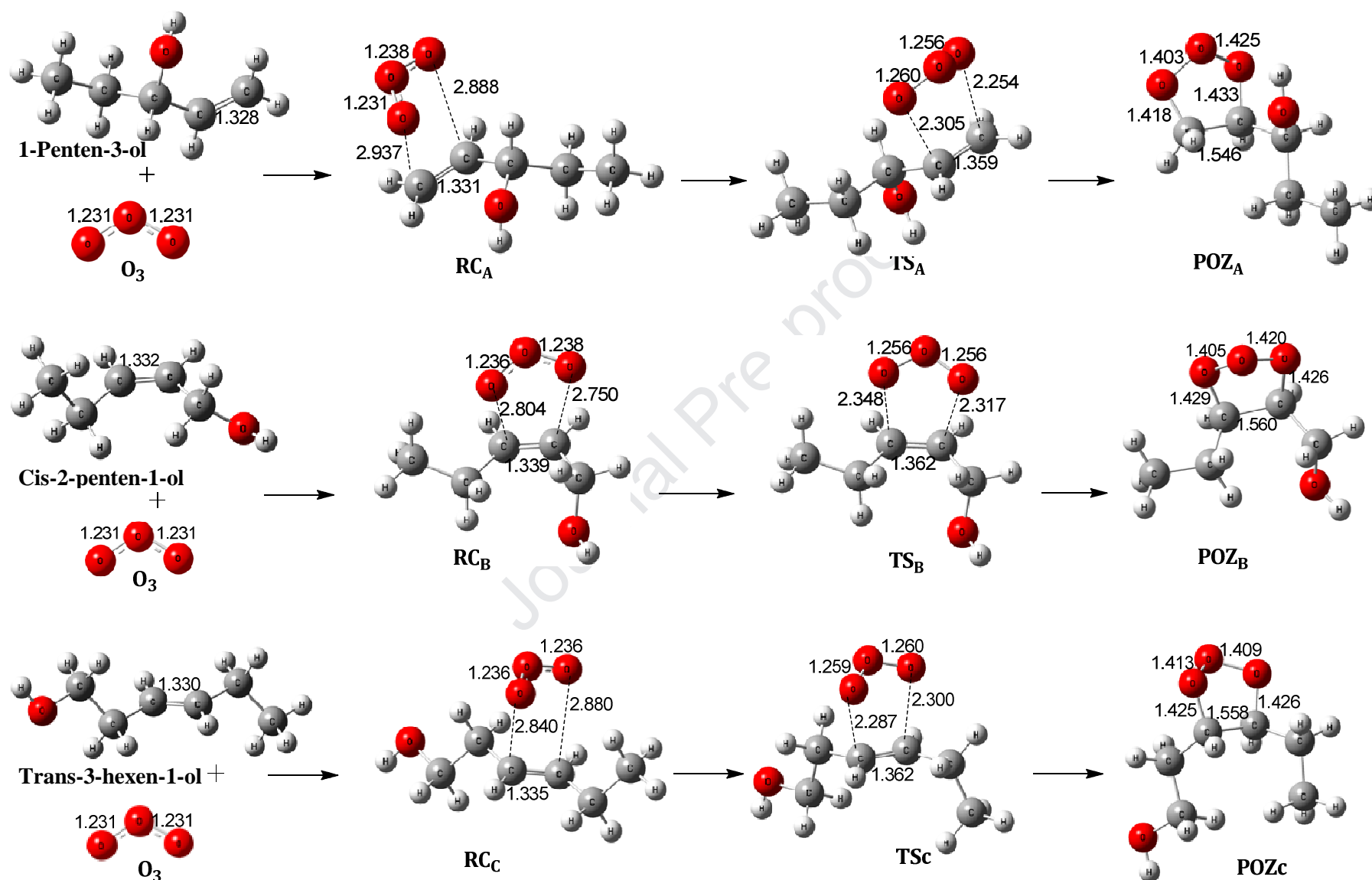


Fig. 5. Optimized geometries of reactants, intermediates, TS, and primary ozonides formed in the reaction of O₃ with A (1-penten-3-ol), B (cis-2-penten-1-ol) and C (trans-3-hexen-1-ol). All are optimized at M06-2x/6-311++G(d,p) level.

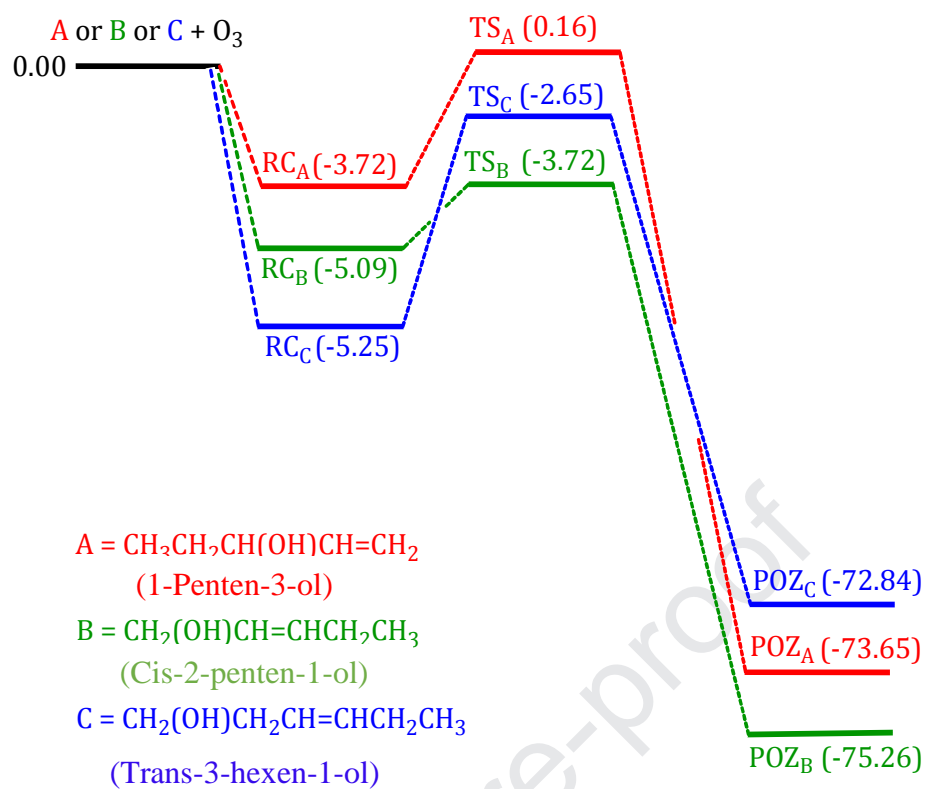


Fig. 6. Energy profile of the reactions of O_3 with the reactants A (red), B (green) and C (blue). Energies are given in kcal/mol.

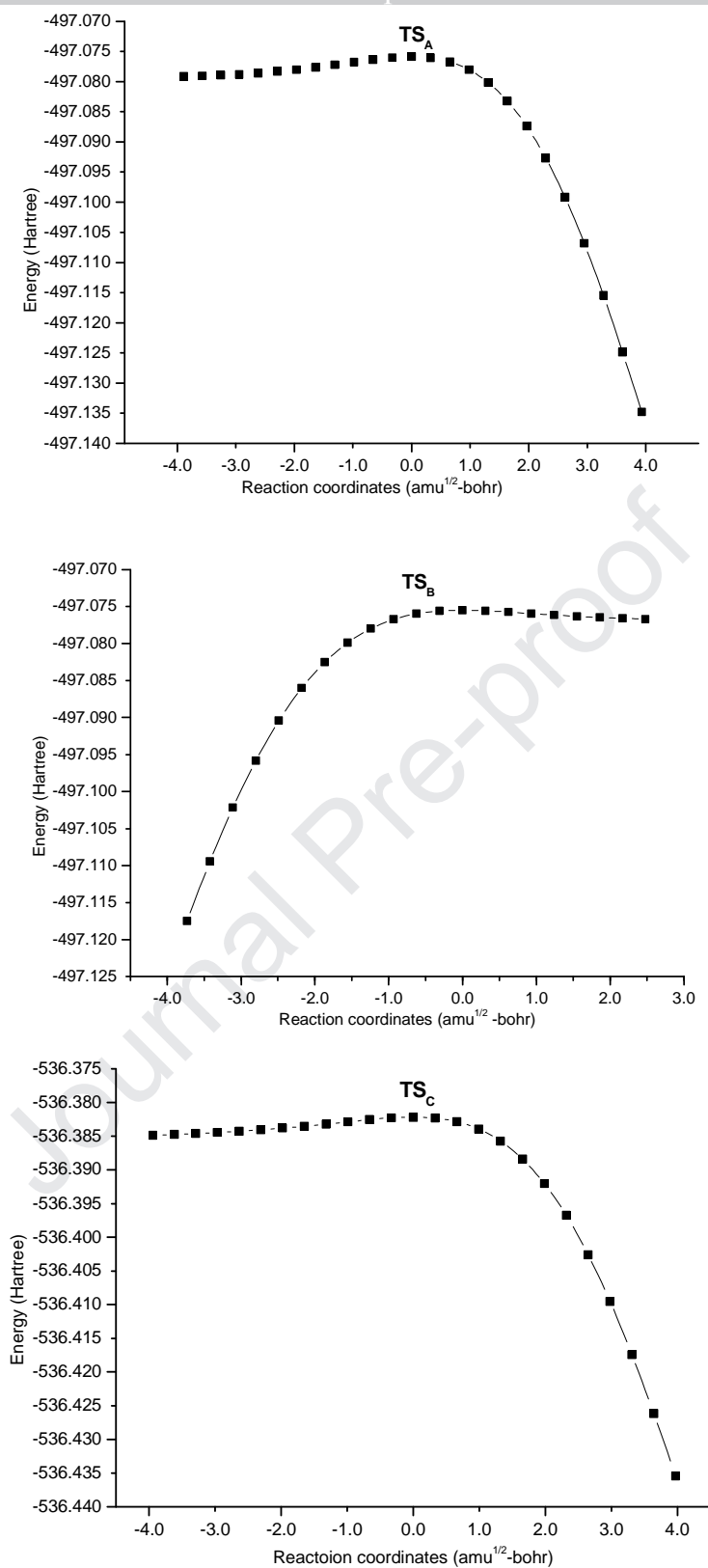


Fig. 7. Intrinsic reaction coordinate (IRC) plots for the TSs of reactions of ozone with A (1-propene-3-ol), B (cis-2-penten-1-ol) and C (trans-3-hexen-1ol).

- Room temperature ozonolysis rate constants of 1-Penten-3-ol, Cis-2-penten-1-ol and Trans-3-hexen-1-ol are 1.68, 10.50 and $6.24 \times 10^{-17} \text{ cm}^3 \text{ molecule}^{-1} \text{ s}^{-1}$, respectively.
- The ozonolysis of the studied unsaturated alcohols shows a low positive temperature dependence.
- Calculations have highlighted the formation of a pre-reaction complex that leads to an activated complex.
- Atmospheric lifetimes of the studied compounds toward ozone are of few hours.

Journal Pre-proof

Declaration of interests

The authors declare that they have no known competing financial interests or personal relationships that could have appeared to influence the work reported in this paper.

The authors declare the following financial interests/personal relationships which may be considered as potential competing interests:

Journal Pre-proof